

Self-similarity and coarsening of three dimensional particles on a one or two dimensional matrix

Jorge Viñals

*Supercomputer Computations Research Institute, Florida State University, Tallahassee, Florida
32306-4052, and Department of Chemical Engineering, FAMU/FSU College of Engineering,
Tallahassee, Florida 32310-6046*

W.W. Mullins

*Department of Materials Science and Engineering, Carnegie Mellon University, Pittsburgh,
Pennsylvania 15213-3890*

(November 11, 2018)

Abstract

We examine the validity of the hypothesis of self-similarity in systems coarsening under the driving force of interface energy reduction in which three dimensional particles are intersected by a one or two dimensional diffusion matrix. In both cases, solute fluxes onto the surface of the particles, assumed spherical, depend on both particle radius and inter-particle distance. We argue that overall mass conservation requires independent scalings for particle sizes and inter-particle distances under magnification of the structure, and predict power law growth for the average particle size in the case of a one

dimensional matrix (3D/1D), and a weak breakdown of self-similarity in the two dimensional case (3D/2D). Numerical calculations confirm our predictions regarding self-similarity and power law growth of average particle size with an exponent $1/7$ for the 3D/1D case, and provide evidence for the existence of logarithmic factors in the laws of boundary motion for the 3D/2D case. The latter indicate a weak breakdown of self-similarity.

I. INTRODUCTION

The purpose of this paper is to re-examine the validity of the hypothesis of self-similarity in coarsening systems in which particles of dimension D_p are intersected by a diffusion matrix of different spatial dimensionality D . The discussion is limited to coarsening driven by interface energy reduction, the particles are assumed to remain spherical (e.g., by surface diffusion), and particle migration is neglected. We focus on two specific cases: three dimensional particles intersected by either a two (3D/2D) or one (3D/1D) dimensional diffusion matrix respectively.

The statistical self-similarity hypothesis with one scaling length asserts that after a possible transient, consecutive configurations of the coarsening structure are geometrically similar in a statistical sense [1,2]. As a consequence, any parameter of the structure that is invariant under a uniform magnification is also independent of time. This hypothesis, together with the laws of boundary motion for a specific system (and their scaling under uniform magnification) are sufficient to obtain the equation of motion for any linear scale of the structure (e.g., the average particle radius $\langle R(t) \rangle$ for an ensemble of coarsening spherical domains).

Self-similarity with a single scaling length as stated above is consistent with conservation of mass (volume) only in systems for which $D_p = D$. Thus conservation of particle mass requires,

$$n_A \langle R^{D_p} \rangle = \frac{\langle R^{D_p} \rangle}{d_{av}^D} = \text{const.} \quad (1)$$

where n_A is the number of particles per unit (general) area of substrate and $d_{av} = 1/n_A^{1/D}$ may be regarded as an average spacing between particles. If self-similarity holds for the particle size distribution, then

$$\langle R^{D_p} \rangle = \text{const.} \langle R \rangle^{D_p} \quad (2)$$

so that Eq. (1) can be written

$$\frac{\langle R \rangle^{D_p/D}}{d_{av}} = \text{const.} \quad (3)$$

Self-similarity with one scaling length requires $\langle R \rangle / d_{av} = \text{const.}$ But according to Eq. (3) this condition holds only if $D_p = D$. Therefore, self-similarity with a single scaling length cannot hold when $D_p \neq D$. Unfortunately, self-similarity with one scaling length was used in a section of Ref. [1] to deduce erroneously exponents of particle size in a 3D/2D and a 3D/1D system ($t^{1/4}$ and $t^{1/5}$ respectively).

If $D_p \neq D$, self-similarity with two scaling lengths (e.g., $\langle R \rangle$ and d_{av}) is still possible and is consistent with Eq. (3). In this case, the self-similarity hypothesis would assert that consecutive configurations of the system are statistically equivalent to those obtained by magnifying the original system using two scale factors, one for particle sizes and a second for inter-particle spacings; the two scale factors are related through Eq. (3) to conserve mass. We shall present evidence that this occurs in the 3D/1D case and leads to a particle growth exponent of $1/7$.

In the 3D/2D system, we will present numerical evidence that a necessary condition for self similarity is not met. This condition, established in Appendix A, shows that if the distribution of reduced particle sizes is scale invariant (which it must be in any self-similar regime), then the ratio of the expected growth rates of any two particles must be scale invariant under magnification. We show numerically that this condition is not met in the case of a configuration with a large number of interacting particles of unequal sizes, randomly distributed in space with a Laplacian concentration field satisfying self-consistently

determined mean field boundary conditions at large distances from the particles.

Support for the existence of self-similarity is quite strong in a large variety of physical systems for which $D_p = D$ (see, e.g., reviews in [3–6]). In the case of three dimensional particles growing by diffusion on a two dimensional substrate (the 3D/2D case), experiments and theoretical investigations have been recently reviewed in [7]. Briefly, the system of coarsening particles reaches (at least approximately) a scale invariant state in which the average particle radius grows in time as $\langle R(t) \rangle \propto t^{1/4}$ [8]. Such a growth law has been also predicted on the basis of mean field analyses [9–12]. We shall present evidence that self-similarity with this growth law cannot be strictly true.

In Section II, we use the law of boundary motion in a coarsening system, together with self-similarity, where applicable, to discuss growth exponents. In Section III, we present numerical evidence that in the 3D/1D system, the particle radii and inter-particle distances scale separately to obey Eq. (3) with $\langle R \rangle \propto t^{1/7}$ and $d_{av} \propto t^{3/7}$. Section IV addresses the 3D/2D case and presents numerical evidence for the existence of a logarithmic factor in the laws of boundary motion that involves ratios of particle sizes to inter-particle distances, and indirect evidence that, contrary to the classical case of coarsening of two dimensional particles on a two dimensional substrate, the logarithmic factor leads to a (weak) breakdown of self-similarity. This breakdown would manifest itself in the existence of effective coarsening exponents that change very slowly in time.

II. SELF-SIMILARITY AND GROWTH EXPONENTS

In this section we present the derivation of the growth exponent for the case $D_p = 3, D = 1$ and discuss the complication that arises in the case of $D_p = 3, D = 2$. The discussion is

based on the following theorem: If the reduced particle size distribution is independent of scale, that is, if

$$n(R, t) = \frac{N(t)}{\langle R \rangle} P(R / \langle R \rangle), \quad (4)$$

where $n(R, t)dR$ is the number of particles per unit “area” in the system with (volume equivalent) radii in dR , $\langle R \rangle$ is the average particle size and $P(x)$, in which $x = R / \langle R \rangle$, is the reduced particle size distribution function, then it is shown in the Appendix that

$$\langle \dot{R} | R \rangle = \frac{d \langle R \rangle}{dt} G(x), \quad (5)$$

where $\langle \dot{R} | R \rangle$ is the expected value of dR/dt for particles of radius R . The expression for $G(x)$ given in the appendix shows that as x increases from zero, G increases from negative values, corresponding to particles that shrink on the average, to positive values corresponding to particles that grow on the average; G vanishes at a value $x = x_c$, corresponding to particles that, on the average, do not change size. Eq. (5) shows that the ratio of the expected value of dR/dt for particles of two different sizes is independent of scale as stated in the introduction. We will use this property (which we will refer to as the ratio test) to argue that the 3D/2D system cannot be strictly scale invariant based on the numerical evidence presented in Section IV.

If self-similarity holds (with one or more scaling lengths), the growth exponent may be determined from the scaling of $d \langle R \rangle / dt$. But Eq. (5) shows that $d \langle R \rangle / dt$ scales as $\langle \dot{R} | R \rangle$ which in turn scales as dR/dt for a single particle. Hence the growth exponent may be determined from the scaling of dR/dt .

To discuss the scaling of dR/dt , we consider for simplicity an ensemble of precipitate particles embedded in a matrix, such that their growth or dissolution is limited by diffusion

of one of the species (solute) through the matrix (the discussion can be easily generalized to other systems in which coarsening is driven by surface free energy reduction [1,2]). Let c be the concentration of solute in the matrix, and assume that c in the matrix is much smaller than the (constant) concentration in the precipitate phase c_p , so that $c_p - c$ can be approximated by c_p [13]. Conservation of solute mass requires that for each precipitate particle,

$$S_{D_p} \frac{dR}{dt} = -\frac{1}{c_p} \int j_n dS, \quad (6)$$

where j_n is the normal component of the solute flux along the outward normal to the surface, S_{D_p} is the surface of a particle of radius R in D_p dimensions and is, for example, $S_{D_p} = \pi^{D_p/2} R^{D_p-1} / \Gamma(D_p/2)$ for a hemisphere, and the integral is taken over the surface of the precipitate particle.

For the 3D/1D case, the collection area over which j_n is nonzero is of microscopic size and independent of scale. Let all particle radii be multiplied by λ . Then the flux j_n scales as a gradient which scales as $1/(\lambda d_{av})$, the factor λ arising from the Gibbs-Thomson equation. But, from Eq. (3) $\lambda^3/d_{av} = \text{const.}$ Hence Eq. (6) shows that $\langle \dot{R}|R \rangle$ scales as λ^{-6} . Therefore, if self-similarity holds, Eq. (5) shows that $d\langle R \rangle / dt$ scales as λ^{-6} , or as $\langle R \rangle^{-6}$ so that

$$\frac{d\langle R \rangle}{dt} = \text{const.} \langle R \rangle^{-6}, \quad (7)$$

which integrates to $\langle R \rangle \propto t^{1/7}$ and $d_{av} \propto t^{3/7}$. Evidence supporting this result is presented in Section III.

To discuss the case of a two dimensional matrix we first present an expression for dR/dt in the spirit of a mean field treatment. Consider a disk of radius R located at the origin, and assume quasi-steady diffusion in the matrix ($\nabla^2 c = 0$), with boundary conditions $c(r =$

$\xi) = c_\xi$ at some cut-off distance away from the center, and

$$c(r = R) = c_0 \left(1 + \frac{\Gamma}{R}\right), \quad (8)$$

at the disk's boundary, where c_0 is the solute concentration in the matrix at coexistence, and Γ is the capillary length. Then the rate of change of volume of the particle is proportional to the gradient of solute at the disk times the particle perimeter or

$$S_{D_p} \frac{dR}{dt} = -\frac{1}{c_p} \int j_n dS = \frac{2\pi D_c c_0 \Gamma a_0}{c_p \ln(\xi/R)} \left(\frac{1}{R_c} - \frac{1}{R}\right), \quad (9)$$

where the concentration $c_\xi = c_0(1 + \Gamma/R_c)$ at the cutoff distance is set so that $dR/dt = 0$ for $R = R_c$, D_c is the solute diffusivity in the matrix and a_0 is a microscopic length that defines the width of the particle's collection area. For the 2D/2D case, self-similarity with one scaling length is consistent with Eq. (9) since ξ/R does not change, and hence the ratio of dR/dt for any two particles as given by Eq. (9) is independent of scale as required by Eq. (5). The result $\langle R \rangle \propto t^{1/3}$ then follows from Eq. (9), self-similarity and Eq. (5).

In the 3D/2D case, self similarity with one scaling length would require ξ to scale as R in Eq. (9). This was assumed by Chakraverty in a mean field treatment with the result $\langle R \rangle \propto t^{1/4}$ which again follows from Eqs. (9) and (5), and self-similarity. If, however, ξ scales as d_{av} , the inter-particle separation, then it must scale in accord with Eq. (3) and therefore ξ/R is no longer independent of scale. It would then follow from Eq. (9) that Eq. (5) cannot hold, and the particle distribution function cannot be of the form (4). We present evidence in Section IV that this is the case, independent of the mean field approximation, and hence that self-similarity cannot hold strictly. We point out, however, that the argument of the logarithm is expected to change slowly in time, and hence the logarithmic factor itself will be changing slowly. Hence, approximate scale invariance could be expected over relatively

long periods of time.

III. THREE DIMENSIONAL PARTICLES ON A ONE DIMENSIONAL MATRIX

We present in this section the numerical solution of a model system comprising spherical three dimensional particles arranged on a closed loop (i.e., a line with periodic boundary conditions at the ends), such that each particle can only exchange mass with its two nearest neighbors. Such a configuration is intended to model diffusion controlled coarsening of three dimensional particles when transport through the matrix takes place preferentially along a line (e.g., along a dislocation line). The model, originally introduced by Hunderi *et al.* [14], is a one dimensional version of the so-called bubble models of grain growth in polycrystalline materials. A mean field solution has shown that coarsening proceeds in a self-similar fashion, and the growth law for the average particle size has been calculated [15]. The one dimensional model has been extended to study the existence of self-similarity when multiple grain orientations and grain boundary anisotropies are allowed [16].

We consider a set of N spherical particles of radii $R_i, i = 1, \dots, N$, forming a linear chain with periodic boundary conditions. Particles are arranged on an evenly spaced grid, such that the initial inter-particle separation is one. The rate of change of each particle radius is given by

$$R_i^2 \frac{dR_i}{dt} = \frac{M}{d_{i,i+1}} \left(\frac{1}{R_{i+1}} - \frac{1}{R_i} \right) + \frac{M}{d_{i,i-1}} \left(\frac{1}{R_{i-1}} - \frac{1}{R_i} \right), \quad (10)$$

where M is a mobility coefficient that sets the time scale appropriate for the microscopic mechanism responsible for diffusion, and $d_{i,i+1}$ and $d_{i,i-1}$ are the distances between particles i and its two nearest neighbors $i + 1$ and $i - 1$ respectively. As the system evolves, some

particles shrink to zero radius and are removed. Therefore the total number of particles N decreases with time whereas both average particle size and average inter-particle distance increase. It immediately follows from Eq. (10) that the total volume of the set of particles, $V = (4\pi/3) \sum_{i=1}^N R_i^3$ is independent of time.

We initially place a large number of particles ($N = 3 \times 10^6$) on a line, and impose periodic boundary conditions $R_{N+1}(t) = R_1(t)$, and $d_{N,1}(t) = d_{1,N}(t)$. The Euler method is used to integrate the system of equations (10) with $M = 1$ and a step size $\Delta t = 5$. The initial condition is a set of randomly chosen radii, uniformly distributed between R_{min} and R_{max} . The value of R_{min} is chosen so that the algorithm is stable, and that no particle with $R > R_{min}$ can shrink to zero radius in Δt . We have further chosen $R_{max} = 10$ arbitrarily. The numerical solution proceeds as follows. Given a configuration at time t , $\{R_i(t)\}, i = 1, \dots, N(t)$, Eq. (10) is iterated once for each particle to yield $\{R_i(t + \Delta t)\}$. Any particle for which $R(t + \Delta t) < R_{min}$ is eliminated, so that only $N(t + \Delta t)$ particles remain. Links are then redefined so that each particle is connected to its two nearest neighbors but preserving their original relative distances. We have studied 420,000 iterations, at the end of which 99053 particles were left. We check the accuracy of the integration by monitoring the total volume of the set of particles. At very early times, a large number of particles are lost and the volume after the first 10,000 iterations decreased by 2.5 %. From then on to the end of the calculation, the total volume only changed by 0.3 %.

Figure 1 shows the scaled distribution of particle radii at three different times. The earlier time is slightly before entering the self-similar regime, the other two are arbitrary times within it. All other later times agree with these two within the size of the symbols, indicating the existence of a self-similar regime. In addition, $\langle R \rangle^3 / \langle d \rangle \simeq 0.0033$ ($\langle d \rangle = d_{av}$) changes

by less than 0.2 % between $t = 10^5$ and the end of the calculation, in agreement with the two-length scaling presented in Section I (Eq. (3)). Figure 2 further shows the distribution of inter-particle distances scaled with the average particle radius to the third power, also consistent with the predictions of Section I with regard to the existence of two scaling lengths.

In summary, even though this model has two independent length scales, namely the characteristic particle size and inter-particle distance, there is an attractor for the evolution in which each distribution function is scale invariant, and each length scale satisfies a well defined relationship in the asymptotic limit of long times (although not proportional to each other). Finally, Fig. 3 shows our best estimate of the exponent n , which is very close to the theoretical prediction of $n = 1/7$.

IV. THREE DIMENSIONAL PARTICLES ON A TWO DIMENSIONAL MATRIX

Self-similarity and the associated growth exponent are considerably more difficult to investigate numerically in this case. Previous numerical approaches in three dimensions have considered configurations comprising a large number of point particles and computed growth rates by direct summation of the Green's function of the Laplace operator [17–19]. We have not used this method because the calculation of the Green's function for given boundary conditions requires infinite sums over the appropriate images, a procedure that does not converge in two dimensions. Furthermore, possible deviations from self-similarity depend logarithmically on time, and hence are very weak. As a consequence, numerical integration of some particular model would require long time spans to unambiguously discriminate between such a dependence and power law growth with some effective exponent. We have

therefore focused on the ratio test, namely on whether the ratio of expected growth rates of particles of different sizes is independent of scale. If the ratio is not independent of scale, then the distribution of particle sizes cannot be scale invariant (i.e., Eq. (4) cannot hold). The generality of this procedure is limited by the specific particle distributions that we use to apply the ratio test. These distributions are not obtained self-consistently by direct solution of a coarsening system. It is therefore conceivable that the failure we find of the ratio test for our distributions might not hold for a coarsening system. However, all our numerical evidence clearly points to logarithmic factors in the law of boundary motion for a two dimensional matrix, and we think it is very unlikely that these factors would cancel for a special class of configurations.

We discuss two cases. First, we present a numerical solution to Laplace's equation in a two dimensional square domain with circular disks of fixed radius and concentration at the corners and periodic boundary conditions; the configuration is equivalent to an infinite square lattice with alternating small and big circles at the lattice sites. The solution establishes that, for this simplified configuration of only two types of interacting particles, concentration fields in the domain do have a logarithmic factor involving ratios of particle sizes to inter-particle distances. Second, we extend this solution to an ensemble of small discs with a far field boundary condition of mean-field type, which is also solved for self-consistently. The same conclusion holds for this analysis.

The results will be analyzed in terms of either $\langle \dot{R}|R \rangle$ directly, or in terms of integrated fluxes to particles which are easier to determine numerically. For the latter purpose we define Q to be the integrated volume flux transferred from all shrinking particles to all growing particles, and $q = Q/N$; other related quantities are defined in section IV B. By definition,

$Q = \int_{R_c}^{\infty} S_{D_p} J(R, t) dR$ (see Eq. (6) for the definition of S_{D_p}). Given the definition of J given in Appendix A (Eqs. (A9) and (A3)), and the result (5), one has, in the self-similar regime,

$$q \propto \langle R \rangle^{D_p-1} \frac{d\langle R \rangle}{dt}; \quad (11)$$

q is constant in the standard 3D/3D case, and inversely proportional to the average particle radius for 2D/2D.

In general, q is a function of the radius and location of the centers of all the particles, and of the position of the center of the outer boundary x_0 (assumed, for example, spherical) and its radius R_0 : $q = q(R_0, R_i; x_0, x_j)$. The function q is a homogeneous function of degree -1 for a two dimensional substrate allowing for capillarity. This follows from the observation that if $c(\vec{r})$ is a solution of Laplace's equation for the original configuration satisfying all boundary conditions, then $(1/\lambda)c(\vec{r}/\lambda)$ is a solution for the configuration scaled up uniformly by λ . Hence all gradients scale as $1/\lambda^2$, and integrated fluxes to each particle and therefore q by $1/\lambda$. Now, starting with a given spatial configuration, consider scaling up all particle radii by a factor s , and all centers of particle positions by a different factor t . Then,

$$q(sR_i; tx_j) = q\left(sR_i; s\frac{t}{s}x_j\right) = \frac{1}{s}q\left(R_i; \frac{t}{s}x_j\right) = \frac{1}{s}f(t/s), \quad (12)$$

where $f(1) = q(R_i; x_j)$, and, for simplicity, we have taken the origin of the outer boundary to lie at $x_0 = 0$. The function f depends on the ratio of s and t only. As a consequence, it is sufficient to consider rescaling particle distances at fixed particle radii ($s = 1$) to obtain the scaling of q , and, if self similarity holds, to obtain the growth law for the average particle size through Eq. (11).

A. Two interacting particles in a Laplacian field

The first case considered is shown in Fig. 4. Two discs of radii R_a and R_b , and concentration c_a and c_b , are placed on the corners of a square lattice of side L with periodic boundary conditions. We have considered the case $c_a = 1, R_a = 3$ and $c_b = -1, R_b = 2$ with values of L ranging from $L = 50$ to $L = 500$. In order to model quasi-static diffusive transport in the matrix Laplace's equation is solved in the interior region subject to the boundary conditions specified at the discs boundaries and periodic boundary conditions otherwise. The computational domain is discretized in N_p evenly spaced elements in each direction. The values of N_p are adjusted for each L in order to obtain a reasonably accurate solution, and range from $N_p = 500$ to $N_p = 2500$. Laplace's equation for the concentration field has been solved with a Successive Over-relaxation (SOR) method with Chebyshev acceleration [20].

Figure 5 shows the dependence of q with L at constant radii and concentration of the particles obtained from the direct solution to Laplace's equation in the square domain. The fit indicates the presence of a logarithmic factor in q in the solution, in agreement with the results of the mean field calculation presented in Section II. It shows, for this simple case, that the function f in Eq. (12) has an approximate logarithmic dependence on its argument t/s . When combined with Eq. (11), the result indicates that the coarsening exponent cannot be strictly $1/4$. Furthermore, since L is proportional to d_{av} , the inter-particle spacing, the results indicate that ξ in the mean field expression (Eq. (9)) is not proportional to R but rather (approximately) to d_{av} . If this is so, it follows that the ratio test cannot be satisfied, the reduced particle size is not scale invariant and strict self-similarity does not hold.

B. Interacting particles in a Laplacian field

To investigate the possibility that the growth rates of individual particles all contain the same logarithmic factor which therefore cancels out when ratios are formed and allows the ratio test to be satisfied, we have extended the calculations to a fairly large collection of small interacting particles. The results reported below again indicate that the ratio test fails and therefore that strict self-similarity does not hold.

For numerical reasons, we have chosen elemental square particles of random side ranging from the grid spacing h to $5h$. This eliminates the need to resolve circular contours, but introduces additional anisotropies (and singularities) into the solution. However, we have verified that both effects are negligible in the range of parameters used in our calculations. Furthermore, $c(r)$ becomes spatially isotropic at distances $\approx 3h$ from the square.

A large collection of such squares ($N = 50$) has been placed at random within the inner fourth of a square lattice of side L . We have randomly assigned the value $c_p = +1$ and $c_p = -1$ with equal probability (see Fig. 6). Laplace's equation for the concentration is solved in the outer region with the boundary condition $c = c_\infty$ (uniform) on the outer boundary. The total flux through the outer boundary $J_\infty = -\int \hat{n} \cdot \nabla c dl$ is then computed. For an arbitrary choice of c_∞ , $J_\infty \neq 0$. An iterative procedure is then performed by adjusting the value of c_∞ until $J_\infty = 0$. Such a procedure is intended to model a system of N interacting precipitate particles embedded in a Laplacian field, chosen, as usual, so that the total mass is conserved.

Once a self-consistent solution for a given L has been found, the linear dimensions of the system are scaled up while keeping h and c_p constants and the entire procedure is repeated.

Figure 7 shows the value of c_∞ as a function of L for the configuration shown in Fig. 6. There is an evident dependence of c_∞ on $\ln L$. The three parameter fit is needed to account for a non-zero value of the average concentration. We have also performed a similar numerical computation involving discs of the same size and fixed concentration (so that the average concentration can be set to zero). A two parameter fit to the resulting function c_∞ vs. L is equally good.

We have repeated all our calculations for the related case that involves a large system with periodic boundary conditions, with the elemental squares being uniformly distributed throughout the entire computational domain. Identical results have been obtained, the details of which will not be presented here.

We apply the ratio test in the following form: Eq. (5) implies that if α and β are any two sets of particles each with specified radii, then the ratio $\langle Q_\alpha \rangle / \langle Q_\beta \rangle$ is independent of scale, where $\langle Q_\alpha \rangle$ is the expected value of the integrated flux to particles in set α , and similarly for $\langle Q_\beta \rangle$. Thus

$$\langle Q_\alpha \rangle = \sum_{i \in \alpha} 2\pi R_i^2 \langle \dot{R}_i | R_i \rangle = 2\pi \langle R \rangle^2 \frac{d \langle R \rangle}{dt} \sum_{i \in \alpha} x_i^2 G(x_i) \quad (13)$$

and similarly for $\langle Q_\beta \rangle$ so that in the ratio, the prefactors to the sum cancel and the sums are independent of scale (x_i here is the reduced particle radius).

Figures 8 and 9 show the results of our investigation for the configuration of Fig. 6. For these cases, it is clear that the ratio test fails. In view of these results, it seems very unlikely that there is a special class of configurations for which the ratio of the expected values of the Q 's for any two subset of particles (each with a specified set of R_i 's) could be independent of scale. If this is so, then the reduced particle size distribution in the 3D/2D system is not

independent of scale and self-similarity does not hold.

We summarize our principle results:

1. When the dimensionality of the precipitate particles and of the diffusion matrix differ, self-similarity with one scaling length is not possible as it violates mass conservation. Scaling with two or more lengths is possible.
2. In the case of three dimensional particles embedded in a one dimensional diffusion matrix, we present evidence of scaling with two lengths; the average particle size $\langle R \rangle$, and the inter-particle spacing $\langle d \rangle$. The growth laws are $\langle R \rangle \propto t^{1/7}$, $\langle d \rangle \propto t^{3/7}$, and the distributions of the corresponding reduced variables become independent of time.
3. If the distribution of reduced particle size $x = R / \langle R \rangle$ is independent of scale, we have shown that the expected growth rate of particles of a given radius factors into a product of a function of time only (i.e., $d \langle R \rangle / dt$) and a function of x only. It follows that the ratio of the expected growth rates of particles of two different sizes, or of two groups of particles of different sizes, is independent of scale. This ratio test becomes a necessary condition for self-similarity.
4. We have presented evidence that coarsening of three dimensional particles connected by a two dimensional diffusion matrix is not self-similar. In particular, we have presented evidence from both mean field arguments and from direct numerical solution of particles in a Laplacian field, that the ratio test fails. The failure is weak (logarithmic) and hence over short periods coarsening may appear self-similar with $\langle R \rangle \propto t^{1/4}$.

ACKNOWLEDGMENTS

The research of JV has been supported by the U.S. Department of Energy, contract No. DE-FG05-95ER14566, and also in part by the Supercomputer Computations Research Institute, which is partially funded by the U.S. Department of Energy, contract No. DE-FC05-85ER25000. WWM is supported by the MRSEC Program of the National Science Foundation, contract No. DMR-9632556.

APPENDIX A: EXPECTED RATE OF CHANGE OF PARTICLE RADIUS

We start from the continuity equation for the particle radius distribution

$$\left(\frac{\partial n}{\partial t}\right)_R + \left(\frac{\partial J}{\partial R}\right)_t = 0 \quad (\text{A1})$$

where $n(R, t)dR$ is the number of particles per unit “area” in the system and $J = n(R, t)u(R, t)$ in which u is the average velocity of particles along the R axis, that is $u = \langle \dot{R} | R \rangle$, or the expected value of dR/dt given the value of R .

Now assume that the particle distribution scales so that

$$n(R, t) = \frac{N(t)}{\langle R \rangle} P(x), \quad (\text{A2})$$

where $P(x)$ with $x = R / \langle R \rangle$ is normalized on x ; thus expressed is a product of functions of t only and x only. We seek the functional forms of J and u .

To this end, we first convert Eq. (A1) to express it in terms of x and t . We have,

$$\begin{aligned} \left(\frac{\partial n}{\partial t}\right)_R &= \left(\frac{\partial n}{\partial t}\right)_x + \left(\frac{\partial n}{\partial x}\right)_t \left(\frac{\partial x}{\partial t}\right)_R \\ &= \left(\frac{\partial n}{\partial t}\right)_x - \frac{x}{\langle R \rangle} \frac{d\langle R \rangle}{dt} \left(\frac{\partial n}{\partial x}\right)_t \end{aligned} \quad (\text{A3})$$

and

$$\left(\frac{\partial J}{\partial R}\right)_t = \left(\frac{\partial J}{\partial R}\right)_t \left(\frac{\partial x}{\partial R}\right)_t = \frac{1}{\langle R \rangle} \left(\frac{\partial J}{\partial x}\right)_t. \quad (\text{A4})$$

Substituting these expressions into (A1) we find,

$$\left(\frac{\partial J}{\partial x}\right)_t = x \frac{d\langle R \rangle}{dt} \left(\frac{\partial n}{\partial x}\right)_t - \langle R \rangle \left(\frac{\partial n}{\partial t}\right)_x \quad (\text{A5})$$

as the equation of continuity in terms of x and t . Now substitute (A3) into the right hand side of (A5) and then add and subtract the term $(d\langle R \rangle / dt)(N / \langle R \rangle)P$ which allows the derivatives to be combined with the result,

$$\left(\frac{\partial J}{\partial x}\right)_t = \frac{d\langle R \rangle}{dt} \frac{N}{\langle R \rangle} \frac{d(xP)}{dx} - P \frac{dN}{dt}. \quad (\text{A6})$$

But $N \langle R^{D_p} \rangle = \alpha N \langle R \rangle^{D_p}$ by virtue of (A2) where α is a constant. Therefore,

$$\frac{1}{N} \frac{dN}{dt} + \frac{D_p}{\langle R \rangle} \frac{d\langle R \rangle}{dt} = 0. \quad (\text{A7})$$

Using this relation allows terms of (A6) to be combined to yield

$$\left(\frac{\partial J}{\partial x}\right)_t = -\dot{N} \left[\frac{1}{D_p} \frac{d(xP)}{dx} + P \right] \quad (\text{A8})$$

which shows that the left hand side is a product of functions of time and x only. This expression may be integrated with the added arbitrary function of time chose to cause J to vanish at infinity. The result is,

$$J = nu = -\dot{N} \left[\frac{x}{D_p} P - \int_x^\infty P(x') dx' \right] \quad (\text{A9})$$

which shows that J and hence u are products of functions of t only and of x only.

One can go farther by solving Eq. (A9) for u and using (A3) again to get

$$u(x, t) \equiv \langle \dot{R} | R \rangle = \frac{d\langle R \rangle}{dt} G(x) \quad (\text{A10})$$

where

$$G(x) = x - \frac{D_p}{P} \int_x^\infty P(x') dx'. \quad (\text{A11})$$

Therefore the decomposition (5) or (A10) is a necessary condition for the scaling assumption of the particle size distribution.

REFERENCES

- [1] W. W. Mullins, J. Appl. Phys. **59**, 1341 (1986).
- [2] W. W. Mullins and J. Viñals, Acta metall. **37**, 991 (1989).
- [3] J. D. Gunton, M. San Miguel, and P. S. Sahni, in *Kinetics of first order phase transitions*, Vol. 8 of *Phase Transitions and Critical Phenomena*, edited by C. Domb and J. Lebowitz (Academic, London, 1983).
- [4] K. Binder, in *Condensed Matter Research Using Neutrons* (Plenum, New York, 1984).
- [5] H. Furukawa, Adv. Phys. **34**, 703 (1985).
- [6] A. Bray, Adv. Phys. **43**, 357 (1994).
- [7] M. Zinke-Allmang, L. Feldman, and M. Grabow, Surface Sci. Reports **16**, 377 (1992).
- [8] G. Carlow and M. Zinke-Allmang, Surface Sci. **328**, 311 (1995).
- [9] B. Chakraverty, J. Phys. Chem. Solids **28**, 2401 (1967).
- [10] M. Speight, Acta metall. **16**, 133 (1968).
- [11] H. Kirchner, Metall. Trans. **2**, 2861 (1971).
- [12] N. Gjostein and P. Wynblatt, in *Progress in Solid State Chemistry* (Pergamon, New York, 1975), Vol. 9, p. 21.
- [13] J. Marqusee and J. Ross, J. Chem. Phys. **79**, 373 (1983).
- [14] O. Hunderi, N. Ryum, and H. Westengen, Acta metall. **27**, 161 (1978).
- [15] W. W. Mullins, Acta metall. **39**, 2081 (1991).

- [16] W. Mullins and J. Viñals, *Acta metall. mater.* **41**, 1359 (1993).
- [17] P. Voorhees and M. Glicksman, *Acta metall* **32**, 2001 (1984).
- [18] P. Voorhees, *J. Stat. Phys.* **38**, 231 (1985).
- [19] J. Yao, K. Elder, H. Guo, and M. Grant, *Phys. Rev. B* **47**, 14110 (1993).
- [20] W. Press, B. Flannery, S. Teukolsky, and W. Vetterling, *Numerical Recipes* (Cambridge University Press, Cambridge, MA, 1986).

FIGURES

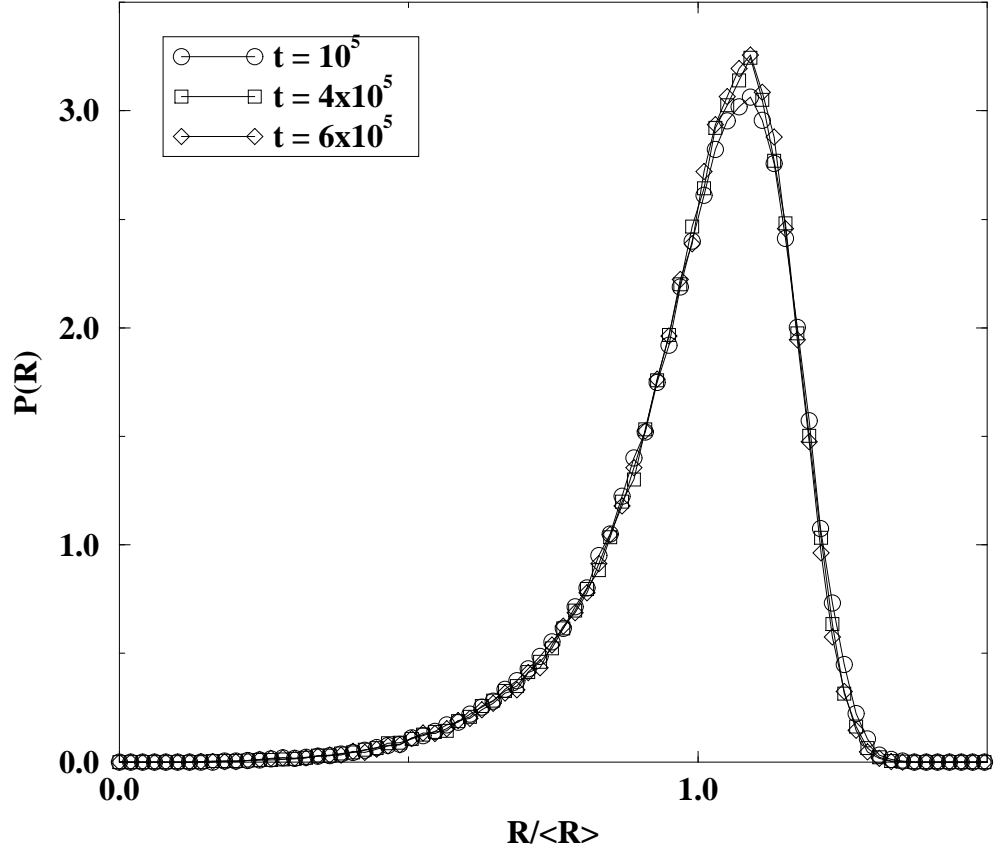


FIG. 1. Scaled distribution of particle radii at three different times as indicated, for three dimensional spherical particles on a line. At the earliest time the system is still approaching a scale invariant state.

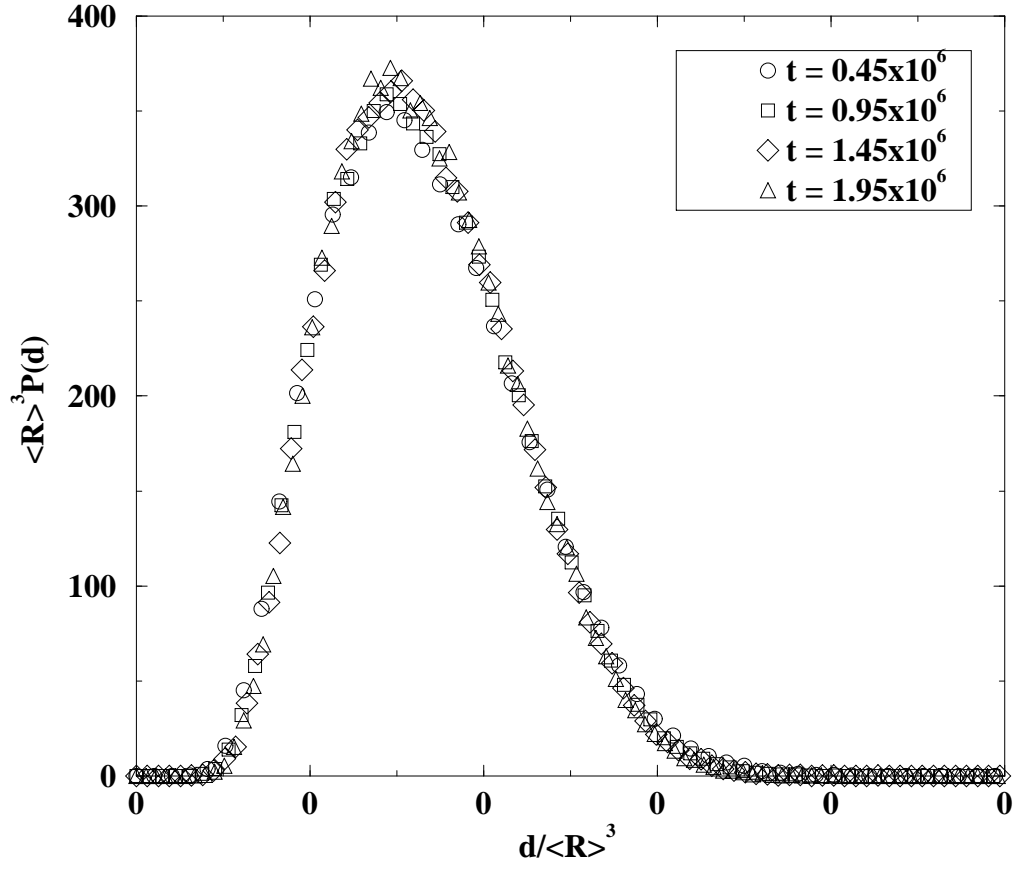


FIG. 2. Distribution of inter-particle separations, $P(d)$, scaled by the average particle size $\langle R \rangle^3$ for the times shown.

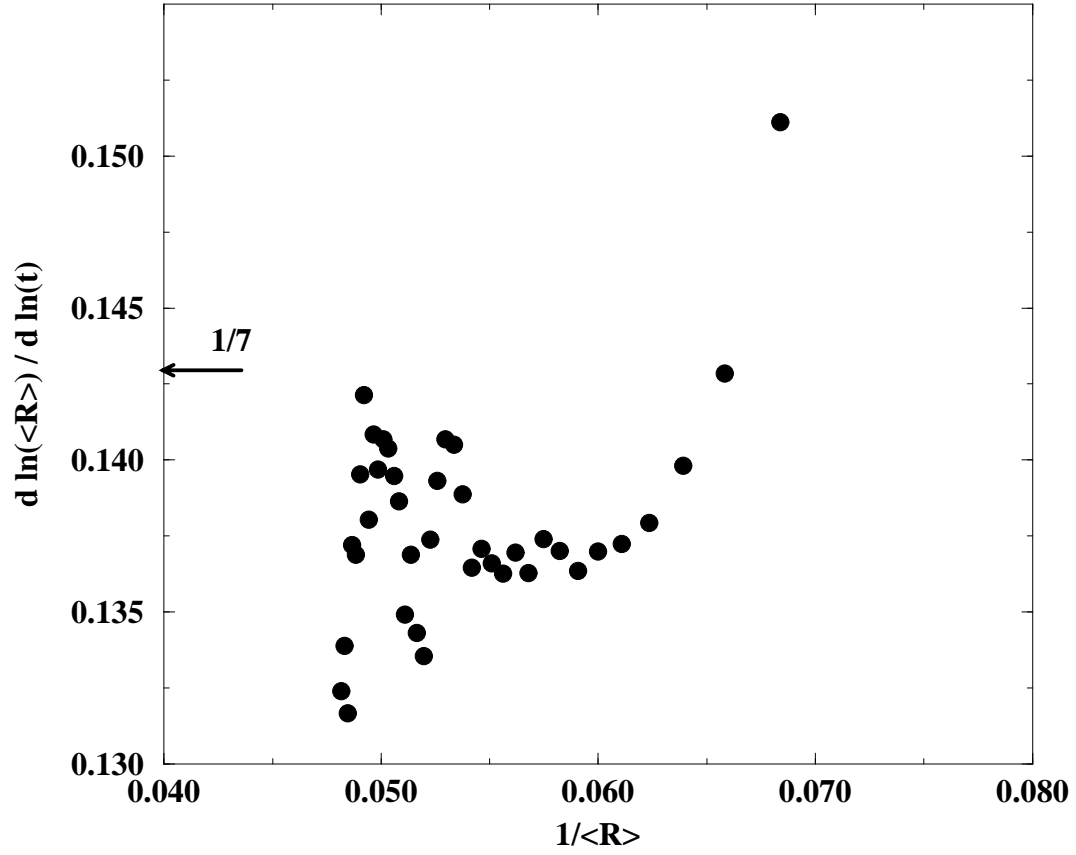


FIG. 3. Logarithmic time derivative of the average particle radius $\langle R \rangle(t)$ plotted versus $1/\langle R \rangle$. For power law growth, the logarithmic derivative asymptotes to a constant equal to the value of the exponent n . The arrow on the left axis indicates the exact position of the value $1/7$.

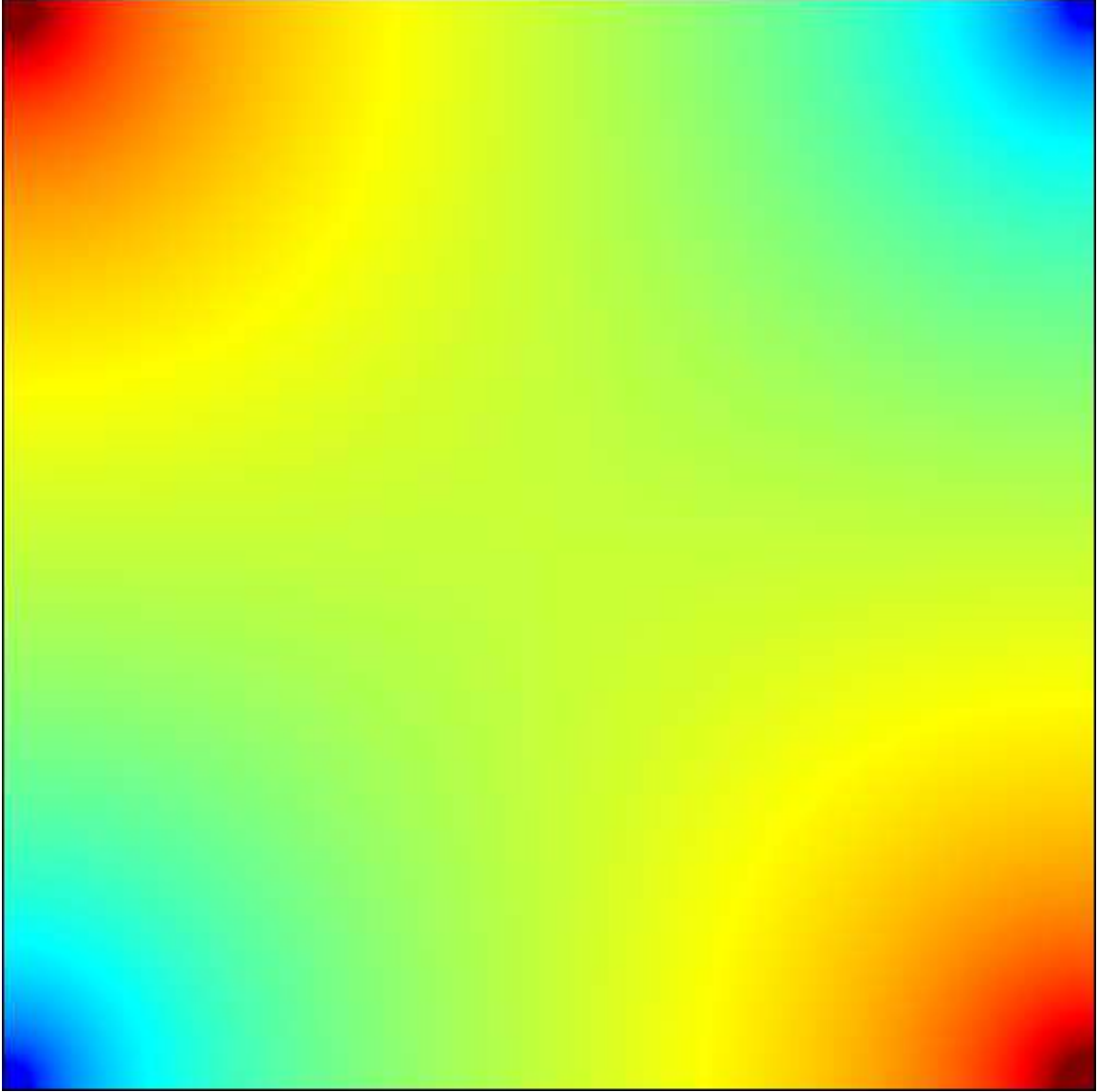


FIG. 4. Two dimensional configuration used in the solution of $\nabla^2 c = 0$; the side of the computational cell is $L = 100$. Two discs of radius $R_a = 3$ (left bottom) and $R_b = 2$ (right bottom) are placed at the corners of the square domain with periodic boundary conditions. The concentration field satisfies Laplace's equation outside the discs, and is constant inside and equal to $c_a = 1$ and $c_b = -1$. We show in grey scale the iso-concentration lines.

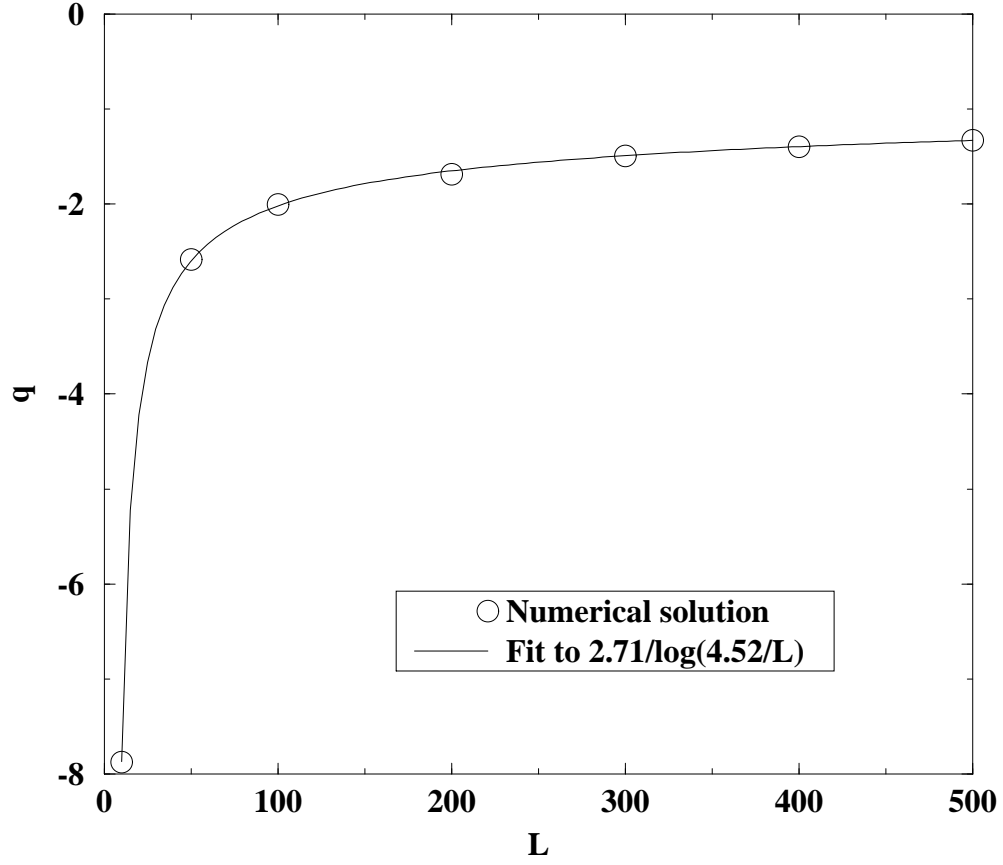


FIG. 5. Average rate of volume transfer from particle b to particle a as a function of the system size L . The remaining parameters have been kept constant and equal $R_a = 3, R_b = 2, c_a = 1$ and $c_b = -1$. The numerical solution is indicated by the circles, and the solid line is a fit to the logarithmic function shown.

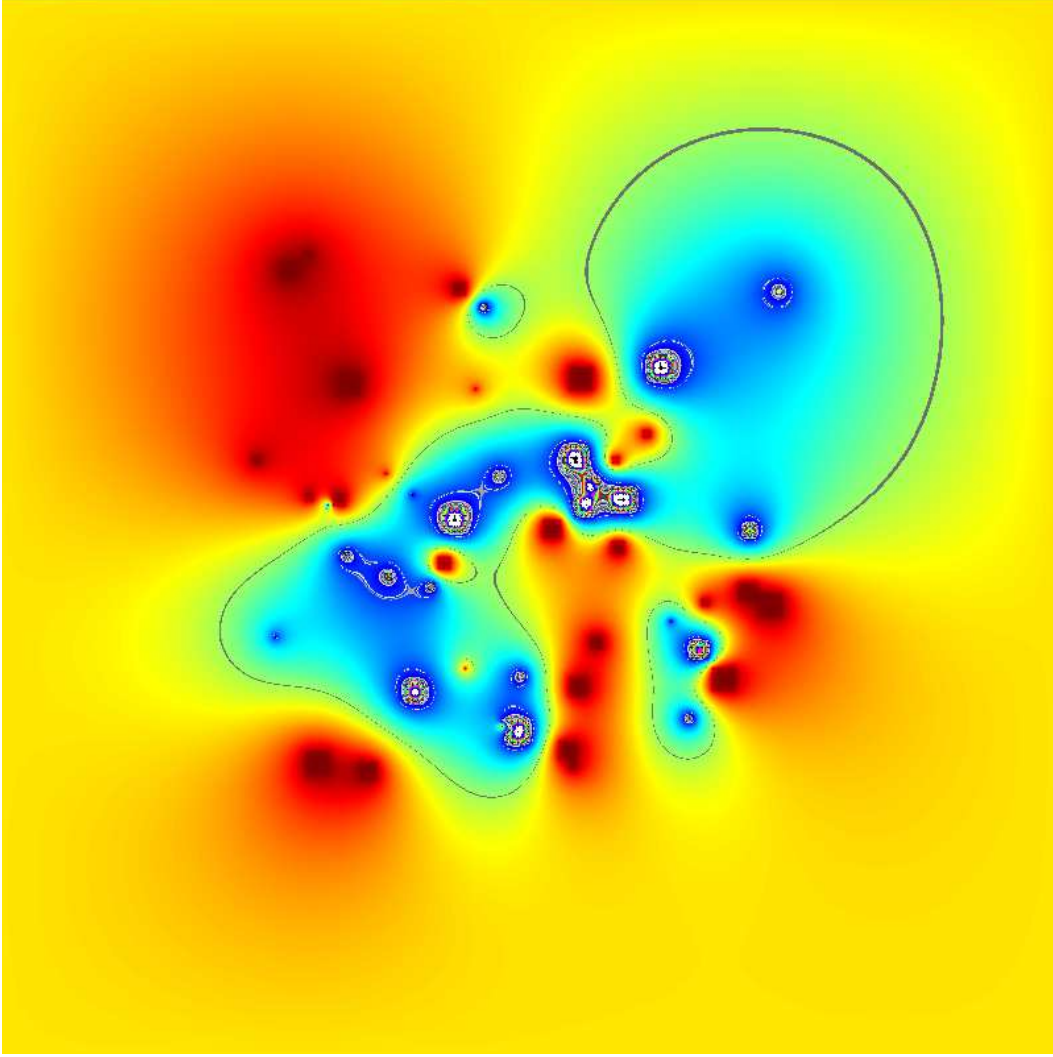


FIG. 6. Example of the configuration used in the numerical solution of $\nabla^2 c = 0$ subject to self-consistent mean field boundary conditions at the outer boundary. Shown are 50 elemental domains of random size (uniformly distributed between h and $5h$, with h the lattice spacing). The composition of each domain is chosen randomly as ± 1 with equal probability. The 50 small elements have been placed at random (uniformly distributed) within the inner quarter of the computational domain. We fix c_∞ at the outer boundary ($x = 0, x = L, y = 0$ and $y = L$) and compute the total flux through this boundary. As described in the text, c_∞ is then adjusted until the total flux vanishes. The solution found is shown in the figure in grey scale.

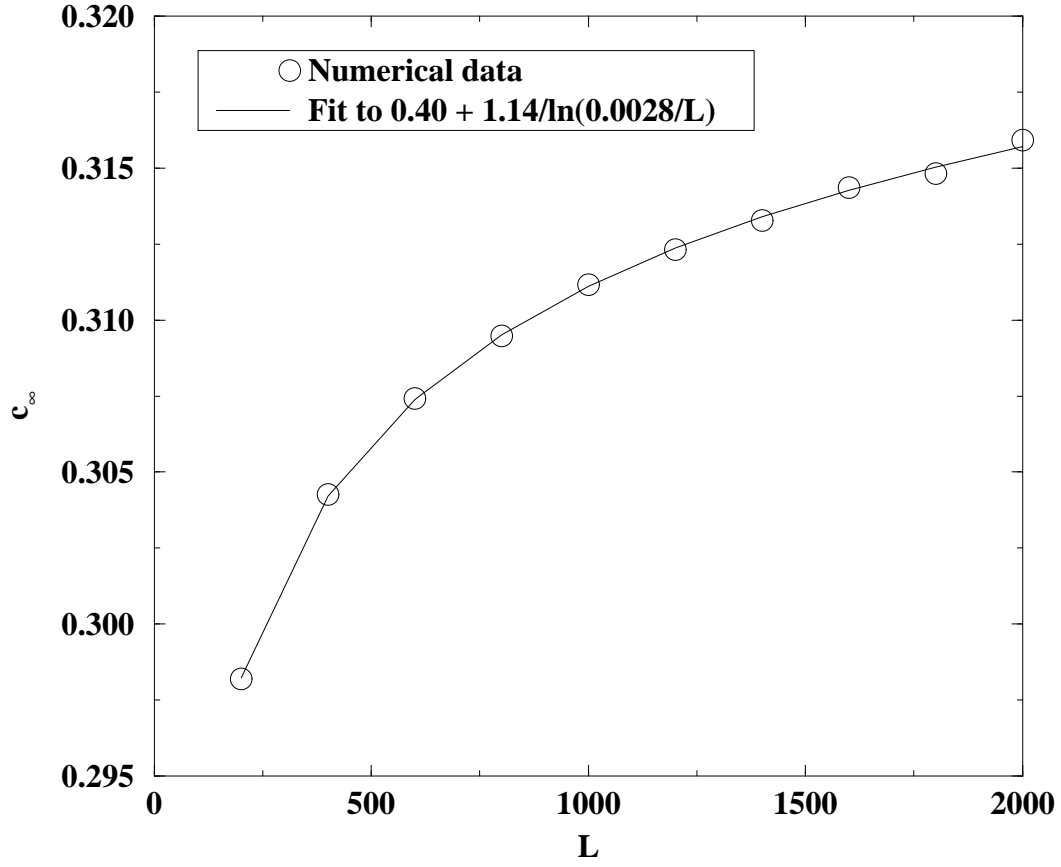


FIG. 7. Mean field concentration c_∞ as a function of system size L for the configuration shown in Fig. 6.

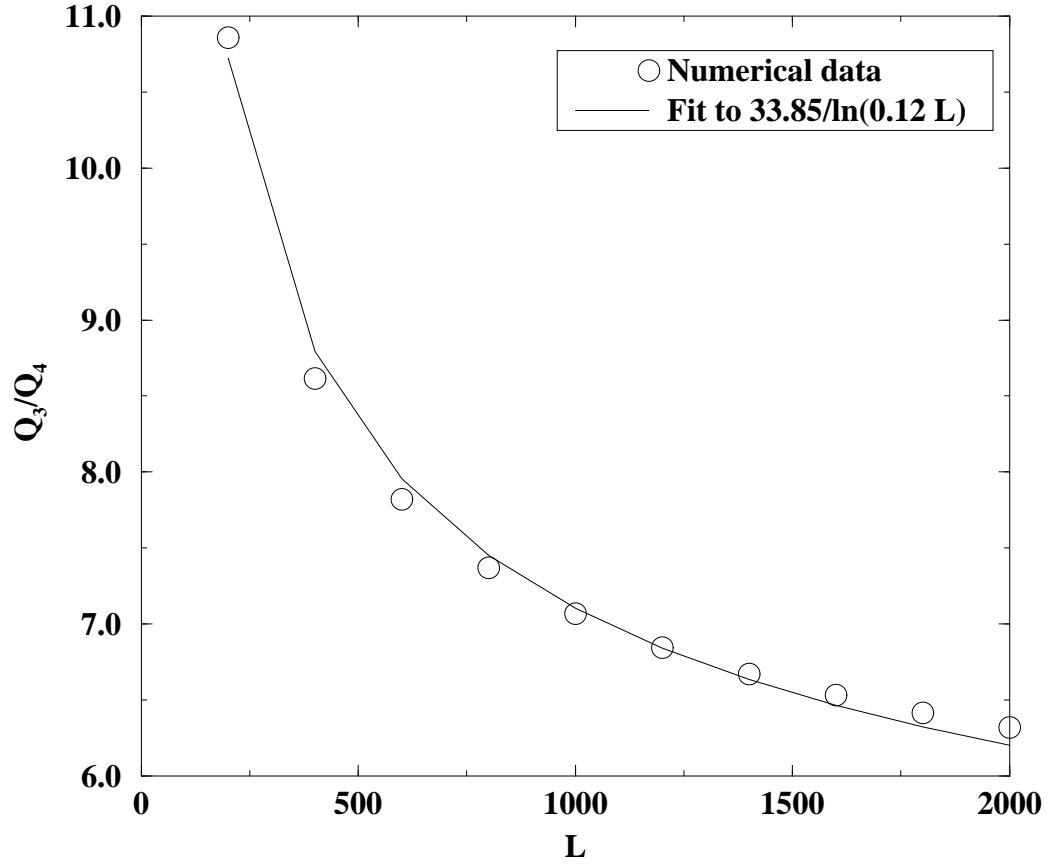


FIG. 8. Ratio test for the configuration shown in Fig. 6. Q_a is the average flux to particles of size ah (the average taken over the configuration). As shown by the figure, the ratio is not independent of L , but includes a logarithmic factor as discussed in the text.

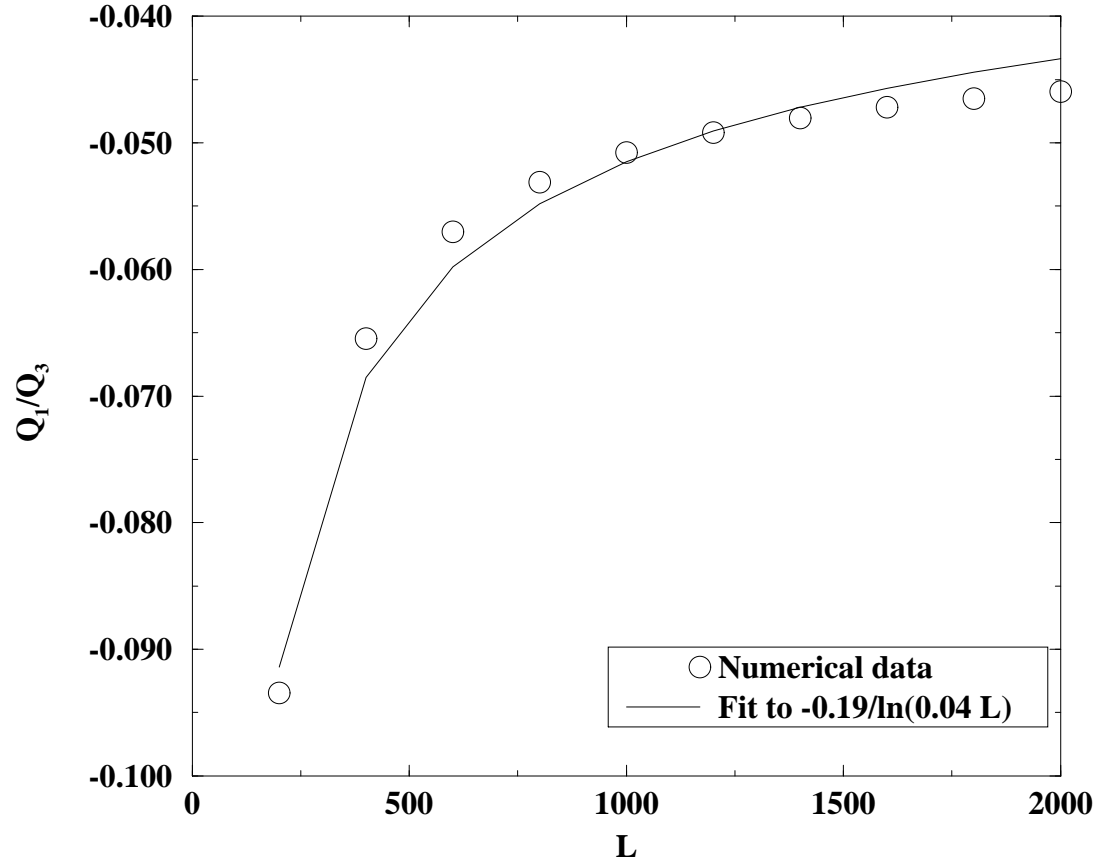


FIG. 9. Ratio test for the configuration shown in Fig. 6. Q_a is the average flux to particles of size ah (the average taken over the configuration).